NANO LETTERS

Letter

pubs.acs.org/NanoLett

Probing Interlayer Interactions in Transition Metal Dichalcogenide Heterostructures by Optical Spectroscopy: MoS_2/WS_2 and $MoSe_2/WSe_2$

Albert F. Rigosi,[§] Heather M. Hill,[§] Yilei Li, Alexey Chernikov, and Tony F. Heinz*[,‡]

Departments of Physics and Electrical Engineering, Columbia University, New York, New York 10027, United States

Supporting Information

ABSTRACT: We have applied optical absorption spectroscopy to investigate van der Waals heterostructures formed of pairs of monolayer transition metal dichalcogenide crystals, choosing MoS_2/WS_2 and $MoSe_2/WSe_2$ as test cases. In the heterostructure spectra, we observe a significant broadening of the excitonic transitions compared to the corresponding features in the isolated layers. The broadening is interpreted as a lifetime effect arising from decay of excitons initially created in either layer through charge transfer processes expected for a staggered band alignment. The measured spectral broadening of 20 meV − 35 meV implies lifetimes for charge separation of the near band-edge A and B excitons in the range of 20−35 fs. Higher-lying transitions exhibit still greater broadening.

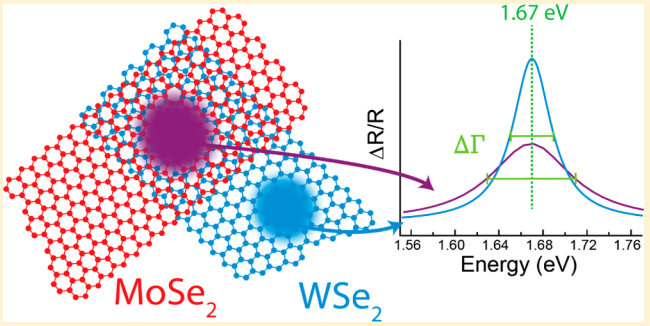

KEYWORDS: *2D materials, heterostructures, transition metal dichalcogenides, lifetime broadening, charge transfer*

The ability to combine semiconducting materials into custom-made heterostructures has enabled both studies of the fundamental properties of electrons in two dimensions (2D) and device applications. Conventional heterostructures, such as quantum-well superlattices, benefit from well-developed growth techniques and from deep understanding of the individual material components. This allows the preparation of materials exhibiting characteristics optimized for a specific application. In this context, 2D van der Waals materials[1−7] offer attractive approaches to the fabrication of heterostructures through the combination of individual layers with sub-nm thickness into tailored multilayered structures. The interfaces of these materials are intrinsically sharp on the atomic scale and, for mechanical assembly, lattice-matching requirements are relaxed because of the weak van der Waals bonding between the layers. This provides great flexibility in the preparation of arbitrary heterostructures, including the possibility of tuning the relative crystallographic orientation of the sheets.[8−12] Such heterostructures draw on a wide variety of possible components such as individual 2D layers. In particular, the semiconducting mono- and few-layers of transition metal dichalcogenides[13−16] (TMDCs) exhibit phenomena ranging from coupling between carrier spin and valley degrees of freedom to efficient light-matter interaction and exceptionally strong many-body effects. The creation of TMDC heterostructures (TMDCHs) and their study is thus a vibrant topic of current research.[17−27]

A central question in this emerging field is how the properties of the heterostructure formed from weakly interacting layers differ from those of the individual crystal layers. Recent reports, primarily concerned with light emission from the heterostructures, have considered the formation of so-called charge transfer states,[18−21] in which photoexcited electrons and holes occupy different layers. For the relevant TMDCHs, the heterostructures are understood to exhibit staggered (type II) band alignment,[28,29] and such charge-separated states will be lower in energy than an exciton formed in either material separately. Evidence for this picture includes the observation of a strong decrease in the luminescence of TMDCHs compared to the individual layers,[17−19,27] a phenomenon ascribed to prompt charge separation, as well as the emergence of new low-lying emission peaks in TMDCHs attributed to radiative recombination of these charge-transfer excitons.[20−23,25] In addition to these spectroscopic signatures of the charge transfer states, a recent study using ultrafast pump−probe spectroscopy provided evidence for very rapid charge transfer processes.[19]

In the present work, we address the issue of the dynamics of interfacial charge separation by means of measurement of the dielectric function of the heterostructure for comparison with the dielectric functions of the individual, separated monolayer components. This approach permits us to track the material's response over a broad spectral range and thus to follow the changes of several excitonic resonances in the TMDCs. We examine as model systems MoS_2/WS_2 and $MoSe_2/WSe_2$ heterostructures formed by the vertical stacking of the

Received: March 17, 2015
Revised: June 17, 2015
Published: July 17, 2015

DOI: 10.1021/acs.nanolett.5b01055
Nano Lett. 2015, 15, 5033−5038

individual monolayers. The dielectric functions of these TMDCHs are found to be approximately what one would expect from a simple superposition of the two respective monolayer constituents. More detailed analysis reveals, however, that although the peak energies and oscillator strengths of the resonances are essentially unchanged, all of the optical transitions are subject to significant spectral broadening in the heterostructures. The origin of the broadening is discussed in the context of both inter- and intralayer scattering processes, as well as of energy transfer processes. Charge-transfer is identified as the dominant process. We note that the broadening places a rigorous lower bound on the charge transfer time. The corresponding time-scale is found to be 20−35 fs, which is consistent with the upper bound on the charge transfer time deduced in recent time-resolved studies of MoS_2/WS_2 TMDCHs.[19]

We prepared TMDCH samples on fused quartz substrates using mechanical exfoliation and mechanical transfer techniques.[3] We first exfoliated crystals of the two parent materials on fused quartz and polypropylene carbonate transferable film. Monolayers were identified by photoluminescence (PL) and Raman spectroscopy, as well as atomic force microscopy (AFM) (see Supporting Information). The TMDCHs were then constructed by transferring MoS_2 onto WS_2 for the sulfur-based heterostructures and, similarly, by transferring WSe_2 onto $MoSe_2$ for the selenium-based heterostructures. All samples were prepared so that the nonoverlapping areas of the monolayers were sufficiently large to be accessed separately in the optical measurements (see micrographs in the Supporting Information). This permitted us to compare the individual monolayers and heterostructures formed from the same exfoliated crystals. The relative crystallographic orientation of the two layers was not controlled, but all results were confirmed for at least three different heterostructures to avoid a chance occurrence of near crystallographic alignment. No meaningful differences were seen for the different samples. The AFM profiles of the TMDCHs confirmed that the monolayers were in direct contact vertically (see Supporting Information).

The optical properties of the samples were probed by reflection measurements. For this purpose, broadband emission from a tungsten halogen lamp was spatially filtered by a pinhole and focused onto the sample with a spot size of about 2−3 μm. The reflected light was then collected by a spectrometer and detected with liquid-nitrogen-cooled CCD camera. All measurements were performed at room temperature. The individual monolayers were measured on the same sample after transfer and under the same conditions as the corresponding TMDCHs.

We characterized the optical response of the individual layers and the heterostructures from the reflectance contrast spectra, $\Delta R/R$. Here, $\Delta R/R = (R_s - R_q)/R_q$, where R_s is the reflectance of the sample on the substrate, and R_q denotes the reflectance of the bare quartz substrate. In the limit of weak reflectance contrast (for the relevant case of a transparent substrate), the reflectance contrast is proportional to the absorption of the sample.[30] Although this relation is very useful for a general understanding of the behavior, in our detailed comparison of the individual layers and the heterostructures, we do not rely solely on this approximation, but carry out a more exact treatment, as discussed below.

Reflectance contrast spectra of the individual monolayers and the corresponding TMDCHs are presented in Figure 1. The monolayer data exhibit the expected spectral features,[15,16,31,32]

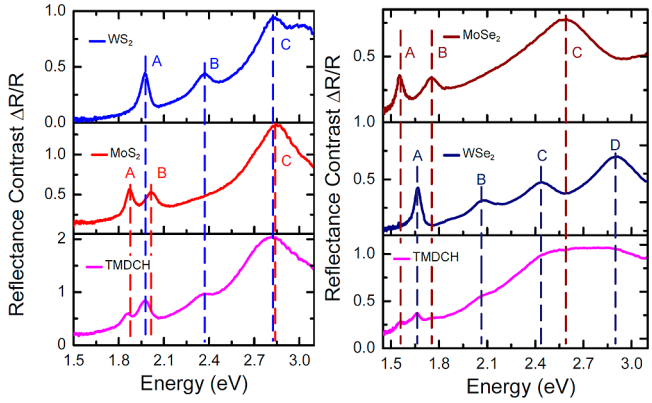

Figure 1. Reflectance contrast measurements for TMDCHs and their constituents, all exfoliated or transferred on fused quartz: (Left) WS_2 and MoS_2, (Right) WSe_2 and $MoSe_2$.

where the lowest-energy (A) peak corresponds to an exciton associated with band-edge transitions at the K and K′ points of the Brillouin zone. The next (B) peak is a similar excitonic transition from the spin split bands, with an energy shift primarily reflecting the valence band splitting.[33] The features above the A and B transition energies, labeled as the C and D peaks, have been proposed as interband transitions mostly occurring in a broad region of the Brillouin zone near the center.[34,35]

For the TMDCHs both the absolute magnitude and peak positions of the optical response resemble a superposition of the corresponding spectra from the two monolayer constituents (Figure 1). We find minor changes in the absolute energies of most resonances. Typically, these shifts lie within the experimental uncertainty of ±10 meV. Redshifts up to 20−30 meV are observed in sulfur-based TMDCHs, particularly for the A exciton peak, but this effect has not been studied systematically.

The direct interaction of electrons in the two layers is expected to be relatively weak for these van der Waals heterostructures, particularly considering that the two layers are not aligned crystallographically. Nonetheless, the lack of significant shifts in the transition energies between the individual layers and the heterostructures might appear surprising in view of the strong many-body effects in these materials[36,37] and the expected modification that these interactions induced by the changed dielectric environment of the heterostructure. We understand the lack of spectral shifts as the consequence of a compensation of two factors: a downward shift in the quasiparticle gap energy through band renormalization combined with a comparable decrease in the exciton binding energy.[38] The same behavior rationalizes the fact that the energy of the band-edge excitonic resonances barely changes in the individual TMDCs with increasing layer thickness.[15,18,31,32,39,40] We also note that there is no evidence of a strong influence of doping or strain on the peak energies.

In contrast to the lack of changes in the position of the optical resonances of the individual materials when the heterostructure is formed, we see that the *widths* of the transitions increase in the TMDCH spectra (Figure 1 and Figure 2). These findings are reproducible for several samples (three or four for each TMDCH system, seven in total, see Supporting Information) with random relative orientation between the individual monolayers in the heterostructure. We thus consider our results typical of an arbitrary misalignment.

DOI: 10.1021/acs.nanolett.5b01055
Nano Lett. 2015, 15, 5033−5038

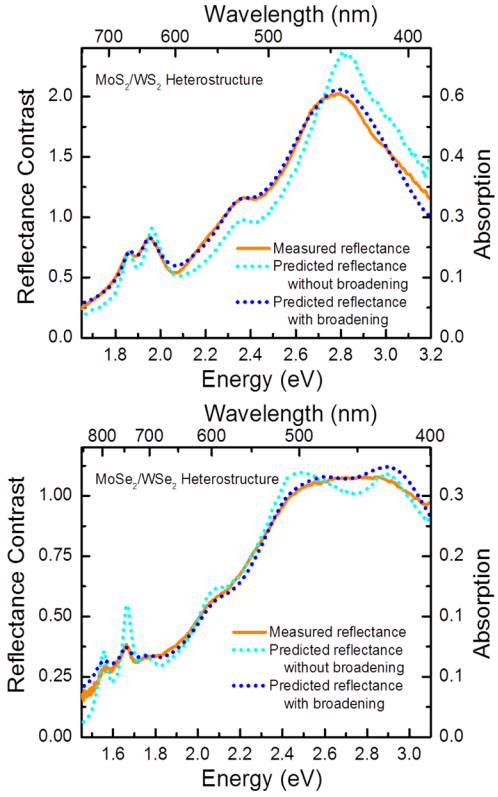

Figure 2. Reflectance contrast spectra of TMDCH as simulated from the dielectric functions of the respective monolayer constituents with (blue dotted line) and without (cyan dotted line) additional peak broadening are compared with the measured data (orange solid line) for (top) MoS_2/WS_2 and (bottom) $MoSe_2/WSe_2$ TMDC heterostructures. Absorption is calculated with the methods in ref 30.

For a more detailed analysis of the data, we first consider a direct superposition of the optical response of the two monolayers combined in a heterostructure. To this end, we extract the dielectric functions for each of the four monolayer TMDCs from the monolayer reflectance contrast measurements via Kramers–Kronig constrained variational analysis.[31] To simulate the optical response of the heterostructures, we then consider a composite medium composed of the two layers, without any modification in the response of either. The effective thickness of the composite medium is given by the sum of the effective thickness of the individual layers and the effective dielectric function is given by the average of the dielectric function of the individual layers, weighted by their respective thicknesses. The expected reflectance contrast spectra produced from this model are shown in Figure 2 for the MoS_2/WS_2 and $MoSe_2/WSe_2$ heterostructures. Comparison of this noninteracting response with the experimental spectra reveals good overall agreement. However, discrepancies are evident, reflecting the broadening of the spectral features previously noted. To quantify these deviations, we parametrize the dielectric functions of the monolayers with a physically meaningful number of Lorentzians, corresponding to the number of peaks observed in the spectral range of interest. In the case of the sulfur-based heterostructure, we parametrize the dielectric function with six Lorentzians, corresponding to three resonances per monolayer. In the case of the selenium-based heterostructure, seven peaks are used since WSe_2 exhibits four resonances in the spectral region of interest (see Supporting Information). It should be noted that the A and B excitons for all four TMDCs are single transitions, thus making the use of a single oscillator appropriate. The single Lorentzian peak for the C feature (and D in the selenium-based TMDCH) is purely a phenomenological description of what is likely to be a more complex set of transitions.[34,35] For our purposes, however, this is adequate to describe the initial response of the individual materials and to characterize the overall degree of spectral broadening.

With this phenomenological characterization of the response of the individual materials, we are able to introduce a broadening of the resonances, while conserving the oscillator strengths (corresponding to the integral of the imaginary part of the dielectric function). The results of this procedure, implemented for both the sulfur-based and selenium-based heterostructures, are presented in Figure 2, with parameters presented in Table 1. We obtain excellent agreement between this simple model and the experimental data. The observed changes in the optical response can be explained purely by spectral broadening, allowing no change in oscillator strengths of the transitions and only slight spectral shifts (~10 meV) in the positions of the resonances when the monolayers are combined to form heterostructures. The one exception is the A transition of MoS_2, whose position was allowed to red-shift up to 25 meV to allow for an optimal determination of the line width broadening.

In both types of heterostructures, the line widths of the A and B excitons increase by about 20–35 meV and the higher-lying C and D transitions by approximately 150 (±60) meV compared with the monolayer constituents. We now examine the physical origin of the observed change in the line width. First, we discuss the influence of impurity broadening. The reflectance data for TMDCHs were compared with the corresponding monolayers measured after the transfer process under exactly the same conditions. Thus, any possible broadening induced by processing is expected to be similar in

Table 1. Exciton Energies Are Shown for the Sulfur and Selenium-Based TMDCH, along with the Change in the Line Width of Those Excitons As Measured on the Heterostructure[a]

feature	energy (±0.01 eV)	ΔΓ (meV)	τ (fs)	feature	energy (±0.01 eV)	ΔΓ (meV)	τ (fs)
MoS_2 A	1.87	26 ± 5	26 ± 5	$MoSe_2$ A	1.56	20 ± 5	33 ± 8
WS_2 A	1.95	21 ± 5	32 ± 8	WSe_2 A	1.67	30 ± 10	22 ± 7
MoS_2 B	2.02	29 ± 10	23 ± 8	$MoSe_2$ B	1.76	20 ± 5	33 ± 8
WS_2 B	2.37	33 ± 10	20 ± 6	WSe_2 B	2.09	25 ± 15	27 ± 16
WS_2 C	2.82	115 ± 20	6 ± 1	WSe_2 C	2.43	60 ± 25	11 ± 5
MoS_2 C	2.86	170 ± 20	4 ± 1	$MoSe_2$ C	2.58	190 ± 35	4 ± 1
WS_2 D	3.06	200 ± 25	3 ± 1	WSe_2 D	2.93	210 ± 40	3 ± 1

[a]The measured changes in line widths (ΔΓ) are then used to deduce an estimate of the exciton lifetime based on the relation: $\tau = \hbar/\Delta\Gamma$.

DOI: 10.1021/acs.nanolett.5b01055
Nano Lett. 2015, 15, 5033–5038

all regions of the sample, including the heterostructure. The overall increase of the line widths is consistent for multiple measurements on the same sample and for TMDCH samples constructed of monolayer components at arbitrary angles with respect to one another (see Supporting Information). The peak broadening thus appears to originate from additional, intrinsic scattering and relaxation channels introduced in the heterostructures. The time scale of the population lifetime τ associated with the observed broadening $\Delta\Gamma$ is estimated from the relation $\tau = \hbar/\Delta\Gamma$ to be on the order of 20−35 fs for both A and B transitions.

We consider intrinsic physical processes underlying the observed increased line width: enhanced thermal phonon scattering in the heterostructure, energy transfer processes between the layers of the heterostructure, and intervalley carrier relaxation either within the same layer or between the two layers. In the following we argue that the last process dominates.

In the TMDC monolayers, the measured line widths of the A exciton transitions are seen to be 50 (±10) meV. The intrinsic contribution to this line width arising from carrier scattering with thermally activated phonons is about 20−30 meV,[41] as estimated from temperature dependent measurements.[41,42] The balance of the experimental line width is attributed to the influence of doping and inhomogeneities and is not expected to change appreciably with respect to the separated layers to the heterostructure, as argued above. With regard to phonon scattering rate, an increase of this rate by a factor of 2, which would correspond to the observed additional broadening in the TMDCHs of 25 (±10) meV, is very unlikely because the scattering of carriers in one layer with the phonons in the adjacent layer should be inefficient in comparison to the scattering within the same layer. In addition, we do not observe any pronounced changes in the Raman scattering intensities: the TMDCH response is nearly a superposition of the two Raman spectra from the individual monolayers (see Supporting Information).

Next, we consider the possible role of energy-transfer processes, that is, the annihilation of an exciton in one layer, creating an exciton in the other. If this relaxation process was dominant, the lowest energy peak in one monolayer forming the TMDCHs (MoS_2 and $MoSe_2$) should not exhibit any significant broadening because the absorption in the companion monolayer is then weak. For the same reason, energy transfer should only produce PL quenching of the higher energy transitions, such as the A excitons in WS_2 and WSe_2. In contrast, we observe similar PL quenching (see Supporting Information) for all four A exciton states of the TMDCHs. Furthermore, estimating the expected time-scale from the energy transfer rates between quantum dots and MoS_2 and for dye molecules on graphene,[43−45] as well as taking into account the $1/R^2$ dependence (shown to be appropriate for the 2D−2D systems in fluorescent polymers[46]), yields a time constant of at least 150 fs. This is about a factor of 5 slower than the sub-50 fs rates inferred from the measured peak broadening. For these reasons the contributions from the energy transfer are also expected to be minor.

This analysis only leaves intervalley scattering of the individual charge carriers as the origin of the observed line broadening in the heterostructures. The most probable scenario for this process is carrier relaxation between the K-valleys in the *opposite* layers. Due to the differences in both their work functions and band gap energies, the band-edges at the K-point in different TMDC monolayers are expected to be offset in energy[47−49] by 100s of meV in a staggered band alignment. Hence, charge transfer of electrons or holes from the K-valley of the one layer to the K-valley of the other is intrinsically favorable with respect to energy, irrespective of which material is initially excited. The emergence of the resulting interlayer PL feature from such a charge transfer exciton has been recently studied in TMDCHs.[18−25] This process is also accompanied by a strong quenching of the intrinsic excitonic emission from the two individual layers[18−21,27] because the charge-transfer competes with the radiative recombination and serves as a fast nonradiative channel for the direct excitons. The magnitude of the quenching typically ranges from about half an order to more than 2 orders of magnitude. In the case of the TMDCHs investigated in this study, we observe a decrease of the excitonic emission by roughly 1 order of magnitude in both the MoS_2/WS_2 and $MoSe_2$/WSe_2 heterostructures (see Figures 1-SI and 2-SI in the Supporting Information), consistent with results in the literature.[18,21]

In the recent study of the charge transfer in such heterostructures by pump−probe spectroscopy, it was shown that the process occurs on a time-scale with an *upper* bound of 50 fs.[19] Because our measurements provide a *lower* bound of 20−35 fs for the time constant of any additional scattering process in heterostructures, it follows that the charge transfer both dominates the lifetime broadening of the A and B excitons and occurs within 20−50 fs.

By way of comparison, time scales for interfacial charge transfer processes investigated in the literature range from 10−100 fs in rare-gas adlayers on metal surfaces and similar systems,[50,51] as well as organic polymer/fullerene blends,[52] to 10−100s of ps in double-quantum wells.[53] Although our measured rates of charge transfer are far faster than those reported for quantum well systems, scaling from the typical thickness regime of quantum wells down to individual monolayers with separations of a few angstroms yields (see Supporting Information) tunneling times on the order of 1 to 10's of femtoseconds for the potential barriers up to several electronvolts. However, as the authors of ref 19 also pointed out, a complete understanding of such fast charge transfer rates is not trivial. One should also consider the role of in-plane momentum for rotationally misaligned layers and the many-body (excitonic) effects on the various the transitions.

Finally, we consider the possibility of intervalley scattering *within individual* layers. This process could play a role in TMDC (twisted) homobilayers, where the coupling between the bands close to the center of the Brillouin zone leads to pronounced shifts of these bands and to the emergence of an indirect band gap.[11,12] Thus, carriers at the K/K′-point in the homobilayers would scatter toward the respective lower-lying valleys after the photoexcitation, leading to a broadening of the exciton resonances. However, for our TMDCHs where two different materials are combined, the bands in the individual layers are not degenerate when combined and weaker interactions are expected. Indeed, recent calculations[47] predict that the K-point resonance remains lower in energy and that no indirect gap emerges from the stacking of two individual layers into heterostructures. This conclusion is supported by the lack of the indirect-gap PL peak at lower energies in our data (see Supporting Information), which in contrast is observed in the twisted homobilayer spectra.[11,12]

In conclusion, we have studied the optical response of MoS_2/WS_2 and $MoSe_2$/WSe_2 TMDC heterostructures over a spectral

DOI: 10.1021/acs.nanolett.5b01055
Nano Lett. 2015, 15, 5033−5038

range of 1.5−3.2 eV using reflectance spectroscopy, tracking both the band-edge and the higher-lying transitions. We find that the optical properties of the TMDCHs can be approximately described by a superposition of the individual monolayer constituents. A detailed analysis shows that though the oscillator strengths of the main transitions are conserved, all resonances are subject to a broadening effect as the monolayers are combined to form heterostructures. The corresponding time constant associated with the additional scattering processes in the TMDCHs is found to be on the order of 20−35 fs for the excitonic A and B transitions in all four materials. Charge-transfer between the layers is identified as a dominant relaxation channel. Our findings are relevant both for the fundamental studies of the interlayer phenomena and for potential applications of TMDC heterostructures in optoelectronic devices.

■ ASSOCIATED CONTENT

Supporting Information

Sample preparation, photoluminescence, Raman spectra, AFM images, and other measurements. The Supporting Information is available free of charge on the ACS Publications website at DOI: 10.1021/acs.nanolett.5b01055.

■ AUTHOR INFORMATION

Corresponding Author

*E-mail: tony.heinz@columbia.edu; tony.heinz@stanford.edu.

Present Address

‡Department of Applied Physics, Stanford University, Stanford, California 94305, United States and SLAC National Accelerator Laboratory, 2575 Sand Hill Road, Menlo Park, California 94025, United States.

Author Contributions

§A.F.R. and H.M.H. contributed equally to this work.

The manuscript was written through contributions of all authors. All authors have given approval to the final version of the manuscript.

Notes

The authors declare no competing financial interest.

■ ACKNOWLEDGMENTS

We would like to thank Tingyi Gu, Ulrich Höfer, Arend van der Zande, Chul-ho Lee, and Philip Kim for fruitful discussions. Support was provided by the National Science Foundation through grant DMR-1124894 and the W. M. Keck Foundation. A.F.R. and H.M.H. acknowledge funding from the National Science Foundation through the Graduate Research Fellowship Program (DGE-1144155) and the Integrated Graduate Education and Research Training Fellowship (DGE-1069240), respectively. A.C. acknowledges partial funding from the Alexander von Humboldt Foundation within the Feodor Lynen Research Fellowship.

■ REFERENCES

(1) Novoselov, K. S.; Jiang, D.; Schedin, F.; Booth, T. J.; Khotkevich, V. V.; Morozov, S. V.; Geim, A. K. *Proc. Natl. Acad. Sci. U. S. A.* **2005**, *102*, 10451.

(2) Wang, Q.; Kalantar-Zadeh, K.; Kis, A.; Coleman, J. N.; Strano, M. S. Electronics and optoelectronics of two-dimensional transition metal dichalcogenides. *Nat. Nanotechnol.* **2012**, *7*, 699−712.

(3) Grigorieva, I. V.; Geim, A. K. van der Waals Heterostructures. *Nature* **2013**, *499*, 419−425.

(4) Butler, S. Z.; Hollen, S. M.; Cao, L.; Cui, Y.; Gupta, J. A.; Gutiérrez, H. R.; Heinz, T. F.; Hong, S. S.; Huang, J.; Ismach, A. F.; Johnston-Halperin, E.; Kuno, M.; Plashnitsa, V. V.; Robinson, R. D.; Ruoff, R. S.; Salahuddin, S.; Shan, J.; Shi, L.; Spencer, M. G.; Terrones, M.; Windl, W.; Goldberger, J. E. Progress, challenges, and opportunities in two-dimensional materials beyond graphene. *ACS Nano* **2013**, *7* (4), 2898−2926.

(5) Das, S.; Robinson, J. A.; Dubey, M.; Terrones, H.; Terrones, M. Beyond Graphene: Progress in Novel Two-Dimensional Materials and van der Waals Solids. *Annu. Rev. Mater. Res.* **2015**, *45*, 1.

(6) Chen, Z.-G.; Shi, Z.; Yang, W.; Lu, X.; Lai, Y.; Yan, H.; Wang, F.; Zhang, G.; Li, Z. Observation of an intrinsic bandgap and Landau level renormalization in graphene/boron-nitride. *Nat. Commun.* **2014**, *5*, 4461.

(7) Ju, L.; Velasco, J.; Huang, E.; Kahn, S.; Nosiglia, C.; Tsai, H.-Z.; Yang, W.; Taniguchi, T.; Watanabe, K.; Zhang, Y.; et al. Photoinduced Doping in Heterostructures of Graphene and Boron Nitride. *Nat. Nanotechnol.* **2014**, *9*, 348−352.

(8) Jariwala, D.; Sangwan, V. K.; Lauhon, L. J.; Marks, T. J.; Hersam, M. C. Emerging Device Applications for Semiconducting Two-Dimensional Transition Metal Dichalcogenides. *ACS Nano* **2014**, *8*, 1102−1120.

(9) Hunt, B.; Sanchez-Yamagishi, J. D.; Young, A. F.; Yankowitz, M.; LeRoy, B. J.; Watanabe, K.; Taniguchi, T.; Moon, P.; Koshino, M.; Jarillo-Herrero, P.; Ashoori, R. C. Massive Dirac fermions and Hofstadter butterfly in a van der Waals heterostructure. *Science* **2013**, *340* (6139), 1427−1430.

(10) Dean, C. R.; Wang, L.; Maher, P.; Forsythe, C.; Ghahari, F.; Gao, Y.; Katoch, J.; Ishigami, M.; Moon, P.; Koshino, M.; Taniguchi, T.; Watanabe, K.; Shepard, K. L.; Hone, J.; Kim, P. Hofstadter's butterfly and the fractal quantum Hall effect in moiré superlattices. *Nature* **2013**, *497* (7451), 598−602.

(11) van der Zande, A. M.; Kunstmann, J.; Chernikov, A.; Chenet, D. A.; You, Y.; Zhang, X.; Huang, P. Y.; Berkelbach, T. C.; Wang, L.; Zhang, F.; Hybertsen, M. S.; Muller, D. A.; Reichman, D. R.; Heinz, T. F.; Hone, J. C. Tailoring the electronic structure in bilayer molybdenum disulfide via interlayer twist. *Nano Lett.* **2014**, *14*, 3869−3875.

(12) Liu, K.; Zhang, L.; Cao, T.; Jin, C.; Qiu, D.; Zhou, Q.; Zettl, A.; Yang, P.; Louie, S. G.; Wang, F. Evolution of Interlayer Coupling in Twisted MoS_2 Bilayers. *Nat. Commun.* **2014**, *5*, 4966.

(13) Wilson, J. A.; Yoffe, A. D. The Transition Metal Dichalcogenides Discussion and Interpretation of the Observed Optical, Electrical and Structural Properties. *Adv. Phys.* **1969**, *18*, 193−335.

(14) Neville, R. A.; Evans, B. L. The Band Edge Excitons in 2H-MoS2. *Phys. Status Solidi B* **1976**, *73*, 597.

(15) Splendiani, A.; Sun, L.; Zhang, Y. B.; Li, T. S.; Kim, J.; Chim, C. Y.; Galli, G.; Wang, F. Emerging Photoluminescence in Monolayer MoS_2. *Nano Lett.* **2010**, *10*, 1271−1275.

(16) Mak, K. F.; Lee, C.; Hone, J.; Shan, J.; Heinz, T. F. Atomically Thin MoS_2: A New Direct-Gap Semiconductor. *Phys. Rev. Lett.* **2010**, *105*, 136805.

(17) Chiu, M.-H.; Zhang, C.; Shiu, H. W.; Chu, C.-P.; Chen, C.-H.; Chang, C.-Y. S.; Chen, C.-H.; Chou, M.-Y. Determination of Band Alignment in Transition Metal Dichalcogenides Heterojunctions. 2014, *http://arxiv.org/abs/1406.5137v1*. arXiv.org e-Print archive. http://arxiv.org/abs/1406.5137v3 (accessed August 2014).

(18) Yu, Y.; Hu, S.; Su, L.; Huang, L.; Liu, Y.; Jin, Z.; Purezky, A. A.; Geohegan, D. B.; Kim, K. W.; Zhang, Y.; Cao, L. Equally Efficient Interlayer Exciton Relaxation and Improved Absorption in Epitaxial and Nonepitaxial MoS2/WS2 Heterostructures. *Nano Lett.* **2015**, *15* (1), 486−491.

(19) Hong, X.; Kim, J.; Shi, S. F.; Zhang, Y.; Jin, C.; Sun, Y.; Tongay, S.; Wu, J.; Zhang, Y.; Wang, F. Ultrafast Charge Transfer in Atomically Thin MoS_2/WS_2 Heterostructures. *Nat. Nanotechnol.* **2014**, *9*, 682−686.

(20) Rivera, P.; Schaibley, J. R.; Jones, A. M.; Ross, J. S.; Wu, S.; Aivazian, G.; Klement, P.; Ghimire, N. J.; Yan, J.; Mandrus, D. G.; Yao, W.; Xu, X. Observation of Long-Lived Interlayer Excitons in

DOI: 10.1021/acs.nanolett.5b01055
Nano Lett. 2015, 15, 5033−5038

Monolayer MoSe2-WSe2 Heterostructures. *Nat. Commun.* **2015**, *6*, 6242.
(21) Fang, H.; Battaglia, C.; Carraro, C.; Nemsak, S.; Ozdol, B.; Kang, J. S.; Bechtel, H. A.; Desai, S. B.; Kronast, F.; Unal, A. A.; et al. Strong Interlayer Coupling in van der Waals Heterostructures Built from Single-Layer Chalcogenides. *Proc. Natl. Acad. Sci. U. S. A.* **2014**, *111*, 6198.
(22) Gong, Y.; Lin, J.; Wang, X.; Shi, G.; Lei, S.; Lin, Z.; Zou, X.; Ye, G.; Vajtai, R.; Yakobson, B. I.; Terrones, H.; Terrones, M.; Tay, B. K.; Lou, J.; Pantelides, S. T.; Liu, Z.; Zhou, W.; Ajayan, P. M. Vertical and in-plane heterostructures from WS2/MoS2 monolayers. *Nat. Mater.* **2014**, *13*, 1135−1142.
(23) Chiu, M.-H.; Li, M.-Y.; Zhang, W.; Hsu, W.-T.; Chang, W.-H.; Terrones, M.; Terrones, H.; Li, L.-J. Spectroscopic Signatures for Interlayer Coupling in MoS2 WSe2 van der Waals Stacking. *ACS Nano* **2014**, *8* (9), 9646−9656.
(24) Liu, K.; Yan, Q.; Chen, M.; Fan, W.; Sun, Y.; Suh, J.; Fu, D.; Lee, S.; Zhou, J.; Tongay, S.; Ji, J.; Neaton, J. B.; Wu, J. Elastic Properties of Chemical-Vapor-Deposited Monolayer MoS2, WS2, and Their Bilayer Heterostructures. *Nano Lett.* **2014**, *14*, 5097−5103.
(25) Tongay, S.; Fan, W.; Kang, J.; Park, J.; Koldemir, U.; Suh, J.; Narang, D. S.; Liu, K.; Ji, J.; Li, J.; Sinclair, R.; Wu, J. Tuning Interlayer Coupling in Large-Area Heterostructures with CVD-Grown MoS_2 and WS_2 Monolayers. *Nano Lett.* **2014**, *14* (6), 3185−3190.
(26) Shim, G. W.; Yoo, K.; Seo, S. B.; Shin, J.; Jung, D. Y.; Kang, I. S.; Ahn, C. W.; Cho, B. J.; Choi, S. Y. Large-Area Single-Layer $MoSe_2$ and Its van der Waals Heterostructures. *ACS Nano* **2014**, *8*, 6655−6662.
(27) Ceballos, F.; Bellus, M. Z.; Chiu, H.; Zhao, H. Ultrafast Charge Separation and Indirect Exciton Formation in a MoS_2−$MoSe_2$ van der Waals Heterostructure. *ACS Nano* **2014**, *8*, 12717.
(28) Kosmider, K.; Fernandez-Rossier, J. Electronic Properties of the MoS_2-WS_2 Heterojunction. *Phys. Rev. B: Condens. Matter Mater. Phys.* **2013**, *87*, 075451.
(29) Komsa, H. P.; Krasheninnikov, A. V. Electronic Structures and Optical Properties of Realistic Transition Metal Dichalcogenide Heterostructures from First Principles. *Phys. Rev. B: Condens. Matter Mater. Phys.* **2013**, *88*, 085318.
(30) Mak, K. F.; Sfeir, M. Y.; Wu, Y.; Lui, C. H.; Misewich, J. A.; Heinz, T. F. Measurement of the optical conductivity of graphene. *Phys. Rev. Lett.* **2008**, *101*, 196405.
(31) Li, Y.; Chernikov, A.; Zhang, X.; Rigosi, A.; Hill, H.; Van Der Zande, A. M.; Chenet, D. A.; Shih, E.; Hone, J.; Heinz, T. F. Measurement of the optical dielectric function of monolayer transition-metal dichalcogenides: MoS2, MoSe2, WS2, and WSe2. *Phys. Rev. B: Condens. Matter Mater. Phys.* **2014**, *90*, 205422.
(32) Zhao, W.; Ghorannevis, Z.; Chu, L.; Toh, M.; Kloc, C.; Tan, P.-H.; Eda, G. Evolution of Electronic Structure in Atomically Thin Sheets of WS_2 and WSe_2. *ACS Nano* **2013**, *7*, 791−797.
(33) Liu, G.-B.; Shan, W.-Y.; Yao, Y.; Yao, W.; Xiao, D. Three-Band Tight-Binding Model for Monolayers of Group-VIB Transition Metal Dichalcogenides. *Phys. Rev. B: Condens. Matter Mater. Phys.* **2013**, *88*, 085433.
(34) Qiu, D. Y.; da Jornada, F. H.; Louie, S. G. Optical spectrum of MoS 2: Many-body effects and diversity of exciton states. *Phys. Rev. Lett.* **2013**, *111*, 216805.
(35) Carvalho, A.; Ribeiro, R. M.; Neto, A. H. C. Band Nesting and the Optical Response of Two-Dimensional Semiconducting Transition Metal Dichalcogenides. *Phys. Rev. B: Condens. Matter Mater. Phys.* **2013**, *88*, 115205.
(36) Qiu, D. Y.; da Jornada, F. H.; Louie, S. G. Optical spectrum of MoS 2: many-body effects and diversity of exciton states. *Phys. Rev. Lett.* **2013**, *111*, 216805.
(37) Mai, C.; Barrette, A.; Yu, Y.; Semenov, Y. G.; Kim, K. W.; Cao, L.; Gundogdu, K. Many-Body Effects in Valleytronics: Direct Measurement of Valley Lifetimes in Single-Layer MoS_2. *Nano Lett.* **2013**, *14*, 202−206.
(38) Spataru, C. D.; Ismael-Beigi, S.; Capaz, R. B.; Louie, S. G. Quasiparticle and excitonic effects in the optical response of nanotubes and nanoribbons. *Top. Appl. Phys.* **2008**, *111*, 195−227.
(39) Chernikov, A.; Berkelbach, T. C.; Hill, H. M.; Rigosi, A.; Li, Y.; Aslan, O. B.; Reichman, D. R.; Hybertsen, M. S.; Heinz, T. F. Exciton Binding Energy and Nonhydrogenic Rydberg Series in Monolayer WS_2. *Phys. Rev. Lett.* **2014**, *113*, 113076802.
(40) Hill, H. M.; Rigosi, A. F.; Roquelet, C.; Chernikov, A.; Berkelbach, T. C.; Reichman, D. R.; Hybertsen, M. S.; Brus, L. E.; Heinz, T. F. Observation of Excitonic Rydberg States in Monolayer MoS2 and WS2 by Photoluminescence Excitation Spectroscopy. *Nano Lett.* **2015**, *15*, 2992.
(41) Wang, G.; Bouet, L.; Lagarde, D.; Vidal, M.; Balocchi, A.; Amand, T.; Marie, X.; Urbaszek, B. Valley dynamics probed through charged and neutral exciton emission in monolayer WSe2. *Phys. Rev. B: Condens. Matter Mater. Phys.* **2014**, *90*, 075413.
(42) Korn, T.; Heydrich, S.; Hirmer, M.; Schmutzler, J.; Schüller, C. Low-temperature photocarrier dynamics in monolayer MoS2. *Appl. Phys. Lett.* **2011**, *99*, 102109.
(43) Prins, F.; Goodman, A. J.; Tisdale, W. A. Reduced Dielectric Screening and Enhanced Energy Transfer in Single- and Few-Layer MoS2. *Nano Lett.* **2014**, *14* (11), 6087−6091.
(44) Swathi, R. S.; Sebastian, K. L. Resonance energy transfer from a dye molecule to graphene. *J. Chem. Phys.* **2008**, *129*, 054703/1−9.
(45) Swathi, R. S.; Sebastian, K. L. Long range resonance energy transfer from a dye molecule to graphene has (distance)(−4) dependence. *J. Chem. Phys.* **2009**, *130*, 086101/1−3.
(46) Hill, J.; Heriot, S. Y.; Worsfold, O.; Richardson, T. H.; Fox, A. M. Controlled Förster energy transfer in emissive polymer Langmuir-Blodgett structures. *Phys. Rev. B: Condens. Matter Mater. Phys.* **2004**, *69*, 041303−1.
(47) Terrones, H.; Lopez-Urias, F.; Terrones, M. Novel hetero-layered materials with tunable direct band gaps by sandwiching different metal disulfides and diselenides. *Sci. Rep.* **2013**, *3*, 1549.
(48) Kang, J.; Tongay, S.; Zhou, J.; Li, J.; Wu, J. Band offsets and Heterostructures of Two-Dimensional Semiconductors. *Appl. Phys. Lett.* **2013**, *102*, 012111.
(49) Gong, C.; Zhang, H. J.; Wang, W. H.; Colombo, L.; Wallace, R. M.; Cho, K. J. Band Alignment of Two-Dimensional Transition Metal Dichalcogenides: Application in Tunnel Field Effect Transistors. *Appl. Phys. Lett.* **2013**, *103*, 053513.
(50) Wurth, W.; Menzel, D. Ultrafast electron dynamics at surfaces probed by resonant Auger spectroscopy. *Chem. Phys.* **2000**, *251*, 141.
(51) Gudde, J.; Hofer, U. Femtosecond time-resolved studies of image-potential states at surfaces and interfaces of rare-gas adlayers. *Prog. Surf. Sci.* **2005**, *80*, 49−91.
(52) Vacar, D.; Maniloff, E. S.; McBranch, D. W.; Heeger, A. J. Charge-transfer range for photoexcitations in conjugated polymer/fullerene bilayers and blends. *Phys. Rev. B: Condens. Matter Mater. Phys.* **1997**, *56*, 4573.
(53) Alexander, M. G. W.; Nido, M.; Ruhle, W. W. Resonant and nonresonant tunneling in GaAs/AlGaAs Asymmetric double quantum wells. *Superlattices Microstruct.* **1991**, *9*, 1.

DOI: 10.1021/acs.nanolett.5b01055
Nano Lett. 2015, 15, 5033−5038